CARBON 61 (2013) 57–62

Available at www.sciencedirect.com

SciVerse ScienceDirect

journal homepage: www.elsevier.com/locate/carbon

Evolution of Raman spectra in nitrogen doped graphene

Zainab Zafar [a], Zhen Hua Ni [a,*], Xing Wu [b], Zhi Xiang Shi [a], Hai Yan Nan [a], Jing Bai [a], Li Tao Sun [b]

[a] Department of Physics, SEU Research Center of Converging Technology, Southeast University, Nanjing 211189, China
[b] SEU-FEI Nano-Pico Center, Key Laboratory of MEMS of Ministry of Education, School of Electrical Science and Engineering, Southeast University, Nanjing 210096, China

ARTICLE INFO

Article history:
Received 10 January 2013
Accepted 24 April 2013
Available online 29 April 2013

ABSTRACT

We present systematical Raman studies of nitrogen doped graphene (NG). Defective graphene by Ar^+ ion bombardment was also studied for comparison. It was found that the defects/nitrogen dopants in NG are not homogenous. Our results also suggest that the G peak position and I_{2D}/I_G ratio cannot be simply used as fingerprint of doping concentration in NG. Both doping and compressive strain (as verified by transmission electron microscope) contribute to the shift of Raman peaks, while both doping and lattice defects contribute to the attenuation of 2D peak. Finally, the nature of defects in NG was probed and found that they are boundary defects. The detail analysis of the evolution of Raman spectra in NG would greatly help on the characterization and future application of this novel material.

1. Introduction

The extraordinary electrical, optical, mechanical, and thermal properties of graphene make it a promising material in various applications, including electronic and optoelectronic devices, composite materials, energy storage devices [1–4]. The modulation of electronic/electrical properties of graphene becomes highly important for electronic devices which require high on/off ratio and selective doping [5]. Theoretical studies have revealed that substitutional doping can alter the Fermi level and introduce a metal to semiconductor transition in graphene [6,7]. Atoms such as nitrogen and boron are ideal candidates as dopants in graphene. Nitrogen doped graphene (NG) have been successfully synthesized by direct synthesis [8–13] and post treatments [14–18], and n-doping properties were reported in electrical measurements [8,14]. The promising applications of NG in electronic devices, oxygen reduction reaction, biosensing, and energy storage devices have attracted great attentions [9,11,14–19].

Different techniques have been used to study NG, with the most commonly used ones are X-ray photo spectroscopy (XPS) [8,11,17,20], scanning tunneling microscopy [10,21] and Raman spectroscopy [10,12,16,20,22,23]. Raman spectroscopy has been widely used to study graphene [24–35]. The intensity of disorder-induced D peak can be used to estimate the amount of defects in graphene, either intrinsic or introduced by plasma/electron beam irradiation [25–28], the intensity ratio of 2D and G peaks (I_{2D}/I_G) is strongly dependent on doping [30], and the shift of G peak position is also a fingerprint of doping concentration [29]. However, previous Raman studies of NG have not acknowledged systematically the effects that affect the features in Raman spectrum, i.e., both doping [29] and strain [31] can induce shift of G and 2D peaks, the intensity ratio of D and D′ peaks ($I_D/I_{D'}$) can be used to probe the nature of defects [32], the I_{2D}/I_G ratio is not only affected by doping but also by lattice defects [33], and the distribution of nitrogen dopants in NG is not homogenous. In view of this, we carried out systematical Raman studies of NG. It was found that both doping and compressive strain contribute to the shift of Raman peaks, and both electron doping and lattice defects contribute to the attenuation of I_{2D}/I_G ratio of NG. This study suggests that the G peak position and I_{2D}/I_G ratio

* *Corresponding author:* Fax: +86 025 52090600x8202.
E-mail address: zhni@seu.edu.cn (Z.H. Ni).
0008-6223/$ - see front matter
http://dx.doi.org/10.1016/j.carbon.2013.04.065

cannot be simply used to estimate the doping concentration in NG. Finally, the $I_D/I_{D'}$ ratio was used to probe the nature of defects in NG.

2. Experimental

NG films were grown on 25 μm Cu foils by chemical vapor deposition (CVD). The cleaned Cu foil was placed in a CVD chamber and heated up to 1000 °C with a 40 sccm flow of H_2. At 1000 °C, CH_4 (60 sccm) and NH_3 (20, 25, and 30 sccm) were introduced simultaneously at a pressure of 160 Pa. After 15 min of growth, the sample was cooled down to room temperature in H_2 atmosphere. The pristine graphene was synthesized by similar route without introducing NH_3. The as-synthesized graphene and NG films on Cu foil were transferred to 300 SiO_2/Si substrates using a standard PMMA transfer procedure [35]. For comparison, defective graphene (DG) was fabricated by micromechanical cleavage of graphite and followed by Ar^+ ion bombardment [28]. The Raman measurements were carried out at room temperature using a LabRAM HR800 micro-Raman system with 514.5 nm excitation and the laser power is kept below 0.5 mW to avoid laser-induced heating. XPS studies were performed using a ESCALAB 250 system (Thermo VG Scientific) with monochromatic Al Kα (hn1/4 1486.6 eV) excitation.

3. Results and discussion

XPS was used to study the incorporation of nitrogen in graphene and determine the C–N bonding configuration. Fig. 1 shows the C1s and N1s spectra of NG. The C1s peak can be fitted with three sub peaks: the main peak at 284.7 eV corresponds to the graphite-like sp^2 structure [19], showing that most of the carbon atoms are arranged in honeycomb lattice, retaining the structure of graphene (as also verified by high resolution transmission electron microscope (TEM) later). The other peaks at 285.9 and 288.9 eV correspond to N-sp^2 C, and N-sp^3 C bonds, respectively [15–17,20]. There are commonly three kinds of bonding configurations for nitrogen dopants in graphene, i.e., Pyridinic N (~398.1–399.3 eV), Pyrrolic N (~399.8–401 eV) and Quaternary N also known as Graphitic N (~401.1–402.7 eV) [11,15–17]. The single Lorentzion N1s peak located at ~400 eV in Fig. 1b indicates that the NG film has pure Pyrrolic N bonding configuration. The Pyrrolic N structure contains pyrrolic 5-memebered rings and the nitrogen atom contributes two lone-pair electrons to the π system [19]. It also contains N–H bonds which Graphitic N and Pyridinic N lack. As nitrogen dopants were introduced during the growth process, the experimental conditions are important to control the type of substitution. The H_2 rich growth condition in our experiment is important for the synthesis of NG with pure Pyrrolic N bonding configuration. The nitrogen atomic concentration is ~3% for NG grown with 25 sccm flow of NH_3 as determined by XPS. It should be noted that this concentration is an average value, as the distribution of nitrogen dopants in graphene is not homogeneous.

Raman spectroscopy as a powerful and non-destructive technique has been widely used to characterize the structure and electronic properties of carbon materials, such as graphite/graphene, carbon nanotubes and diamond like carbon. Fig. 2 shows typical Raman spectra of pristine graphene, DG by Ar^+ ion bombardment and NG. The pristine graphene presents two intense Raman features, which are assigned to G (~1580 cm^{-1}) and 2D (~2675 cm^{-1}) peaks [34]. In addition to these two peaks, NG and DG present a strong D peak located at ~1348 cm^{-1}, which is activated by defects, i.e., in-plane substitution heteroatoms, vacancies, or grain boundaries/edges [24], through an intervalley double resonance Raman process. The appearance of D peak in NG (I_D/I_G = 1.25) and DG (I_D/I_G = 1.3) indicates that there are similar numbers of defects in these two samples, due to the substitution of nitrogen dopants and the introduction of vacancies during ion bombardment. An additional peak located at ~1620 cm^{-1} (D′ peak) is also observed for NG and DG, which originates from the intravalley double resonance scattering process [24]. However, the D′ peak of NG is more prominent compared to that of DG; in the other words, $I_D/I_{D'}$ is smaller for NG with similar amount of defects. This is related to different natures of defects in NG and DG and will be discussed in detail later. Previous studies have revealed that the intensity of 2D peak is sensitive to lattice defects and doping in graphene [33]. The intensity of 2D peak of pristine graphene is much higher than those of NG and DG, and I_{2D}/I_G of DG is much larger compared to that of NG with similar amount of defects. The effects of lattice defects and doping on the intensity of 2D peak will be discussed later too.

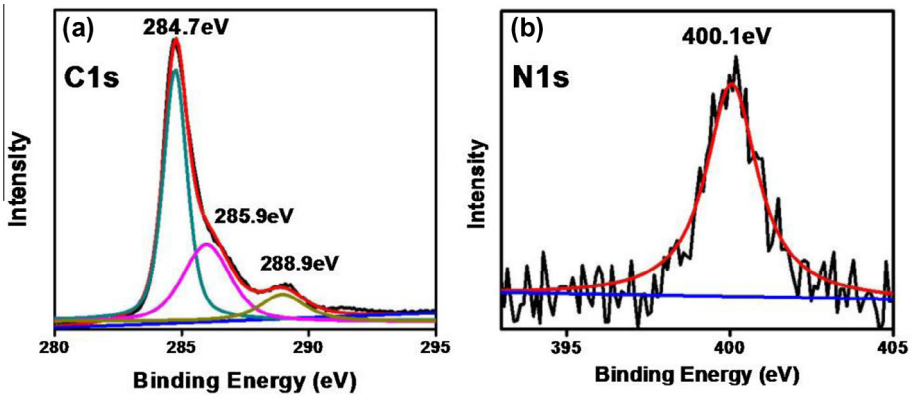

Fig. 1 – XPS C1s (a) and N1s (b) spectra of NG.

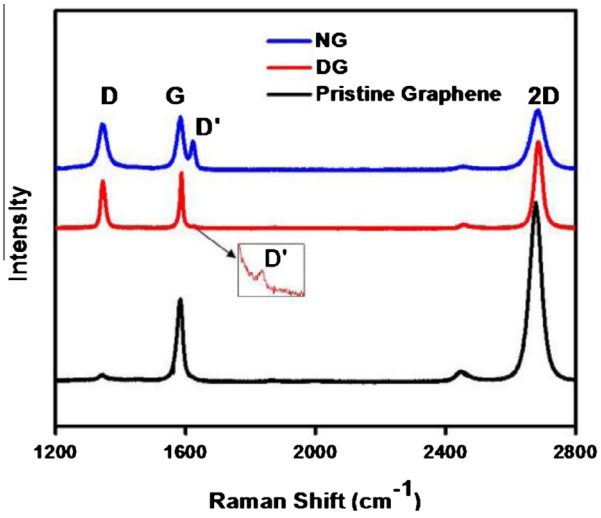

Fig. 2 – Typical Raman spectra of pristine graphene, DG and NG.

The optical image of NG on a 300 nm SiO_2/Si substrate is shown in Fig. 3a. The graphene film is continuous and single layer as confirmed by contrast spectrum [36]. The red box in Fig. 3a represents the area where Raman images were taken. The high resolution TEM image in Fig. 3b reveals the hexagonal arrangement of carbon atoms and indicates the high quality of NG sample. Raman spectra taken from three points of the sample (correspond to points A, B, and C in Raman images) are presented in Fig. 3c. Although the intensities of G peak are similar, the I_D/I_G ratios for points A, B and C are 1, 0.7, and 0.4, respectively. This suggests that the distribution of nitrogen dopants in NG is not homogeneous. Fig. 3d–g present the Raman images generated by the intensities of G, D, D′ and 2D peaks. The distribution of G peak intensity in Fig. 3d further demonstrates the uniformity of NG film. From Fig. 3e, it can be clearly seen that the defects in NG created by nitrogen substitution (I_D) are not homogeneous and have domain-like distribution. The size of domain is commonly around several microns. Such domain-like distribution of nitrogen dopants could be related to the single-crystal domain size of CVD graphene and need to be further studied. The intensity of D′ peak has similar distribution as that of D peak (Fig. 2f), while that of 2D peak (Fig. 2g) has opposite behavior. The D and D′ peaks are activated by inter-valley and intra-valley double resonant Raman process, in which the defects provide the missing momentum in order to satisfy the resonant process. The intensities of both peaks increase with the increase of defect concentration. On the other hand, the 2D peak originates from a two-phonon double resonant process and it does not need defects to fulfill the resonant condition [24]. The intensity of 2D peak is strongly affected by the electron/hole scattering rate [33]. The nitrogen dopants in graphene lattice would create defects in the lattice as well as introduce electron doping [10,21]. Both effects would increase the electron scattering rate and hence the intensity of 2D peak decreases with the increase of defect/dopant concentration.

Fig. 4 shows the changes of $I_{D'}/I_G$ (a) and I_{2D}/I_G (b) with the increase of defect/dopant concentration (I_D/I_G). As can be seen, $I_{D'}/I_G$ increases, while I_{2D}/I_G decreases almost linearly with the increase of I_D/I_G. Fig. 4c and d show another important observation. The G and 2D peaks shift to higher frequencies compared to pristine graphene. The highest amount of blueshift is ~9 cm^{-1} and ~15 cm^{-1} for G and 2D peaks, respectively. There are several possible origins for the shift of Raman peaks, including the effects of doping [29] and strain [31]. The electron/hole doping in graphene affects the interaction between optical phonons and the Dirac fermions transitions across the zero bandgap of graphene. Hence, the G band phonon shows a stiffening as well as bandwidth sharpening with doping. For 2D peak, the influence of dynamic effects is very weak and it is only affected by the modification of the equilibrium lattice parameter with a consequent stiffening/softening of the phonons, with hole doping resulting in a blueshift, and the opposite is true for electron doping [29].

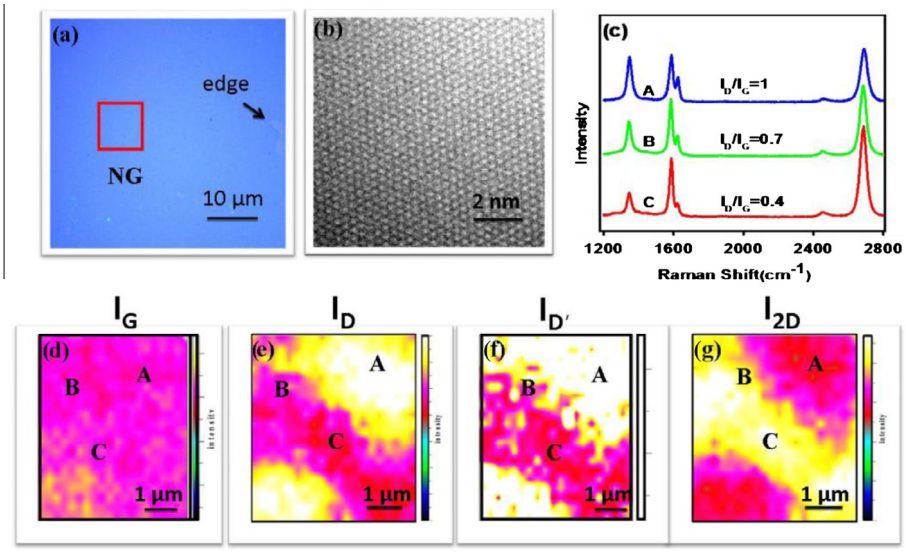

Fig. 3 – (a) Optical image of NG on SiO_2/Si substrate. (b) High resolution TEM image of NG. (c) Raman spectra of NG taken from points A, B, and C in the Raman images. Raman images generated from the intensities of G (d), D (e), D′ (f) and 2D (g) peaks.

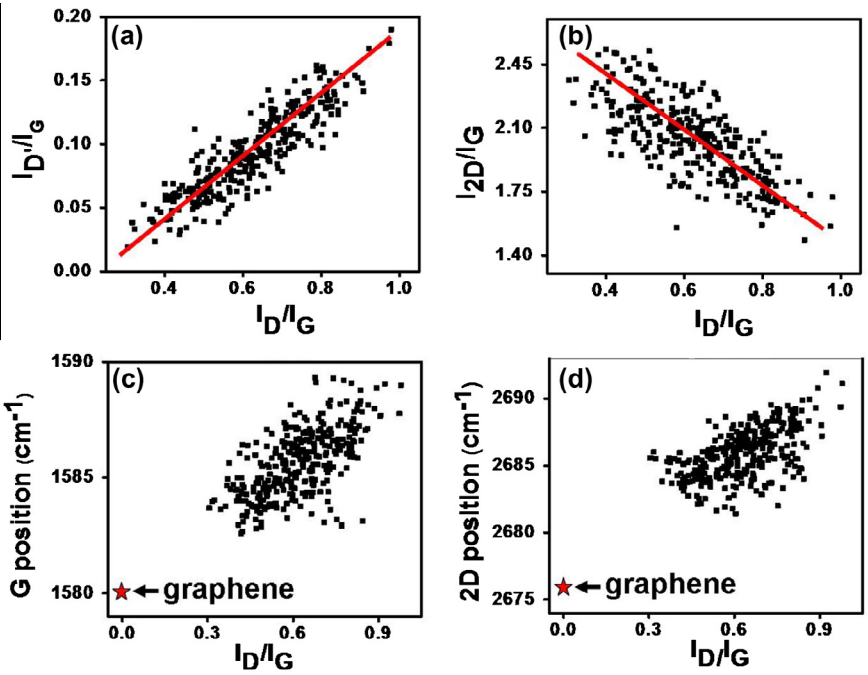

Fig. 4 – Evolution of $I_{D'}/I_G$ (a), I_{2D}/I_G (b), G peak position (c), and 2D peak position (d) with the increase of I_D/I_G. The red stars indicate the peak positions of pristine graphene. (For interpretation of the references to color in this figure legend, the reader is referred to the web version of this article.)

Nitrogen doping was found to introduce n-doping in graphene and carbon nanotubes [10,14,37], and hence should cause a blueshift of G peak and redshift of 2D peak [37] (or no obvious 2D peak shift as presnted by Das et al. [29]). Therefore, the strong blueshifts of G and 2D peaks observed in our case cannot be explained by electron doping only and there should be other mechanisms. It is well known that compressive/tensile strain in graphene could induce a blue/red shift of Raman peaks [31,38]. Substitution of nitrogen atoms in graphene lattice would causes distortion of the lattice and defect pinning [19]. Dettori et al. reported that defects, if associated with bond reconstruction, produce deformation and stress fields [39]. The Pyrrole-like nitrogen forms pentagonal rings in the hexagonal mesh of the graphitic structure, which would introduce stress in the system. Calculations also predict that the distance between adjacent carbon atoms in plane C–C is 1.42 Å, and for a typical Pyrrolic N the length of C–N bond is ~1.37 Å [40]. The shortening of the N–C bond compared to C–C bond suggests that NG might be subjected to compressive strain. Another source of strain is from Cu substrate, Yu et al. revealed that there is ~0.4% compressive strain in CVD graphene prepared at ~1000 °C due to different thermal expansion of Cu and graphene [41]. We have also measured the Raman spectrum of NG directly on Cu substrate and an even larger blueshift of 2D peak was observed (~2710 cm^{-1} as compared to 2676 cm^{-1} of pristine graphene, results not shown), which suggests that the compressive strain induced by Cu substrate does exist and it may not be fully released after transfer. The electron-diffraction patterns of NG by TEM are shown in Fig. 5a. It exhibits hexagonal symmetry with the lattice constant $d = 2.40 \pm 0.02$ Å, while that of pristine graphene is $d = 2.46 \pm 0.01$ Å. This again confirms the present of compressive strain in NG. According to the above analysis, the blueshift of G and 2D peaks in NG is contributed together by electron doping and compressive strain. The scattered data in Fig. 4c and d is another evidence of this combined effect, which is related to the inhomogeneous distribution of dopants and strain in NG.

Apart from the position of G and 2D peaks, the I_{2D}/I_G ratio is also affected by different issues. The intensity of 2D peak is strongly depended on the electron/hole scattering rate (2Γ), which is affected by lattice defects as well as charge carrier doping [33]. The former one would increase the electron-defect elastic scattering rate, while the later one would increase the electron–electron inelastic scattering (Columb interaction) rate. To study the contribution of both effects, I_{2D}/I_G of NG and DG is plotted with the increase of I_D/I_G in Fig. 6a. As can be seen, with similar amount of defects, I_{2D}/I_G of NG is much weaker than that of DG. The attenuation of I_{2D}/I_G for NG with the increase of defect concentration is also much more rapid than that of DG. Different from DG which only creates lattice defects, the nitrogen dopants in NG can also introduce electron doping in the system, i.e., 0.5 carrier per nitrogen atom [21]. Our previous work has reported that a small amount of doping can cause great attenuation of 2D peak [30]. Therefore, the intensity of 2D peaks in NG is much weaker than that of DG due to the extra scattering effect from the nitrogen induced electron doping. Our results suggest that it is inappropriate to simply use the blueshift of G peak and the I_{2D}/I_G ratio to estimate the doping concentration in NG [10,16,20].

Recently, the nature of defects in graphene was probed by Raman spectroscopy by using the $I_D/I_{D'}$ ratio. Different types of defects can be introduced in graphene, i.e., vacancy-like defects can be introduced by Ar^+ bombardment, sp^3 defects

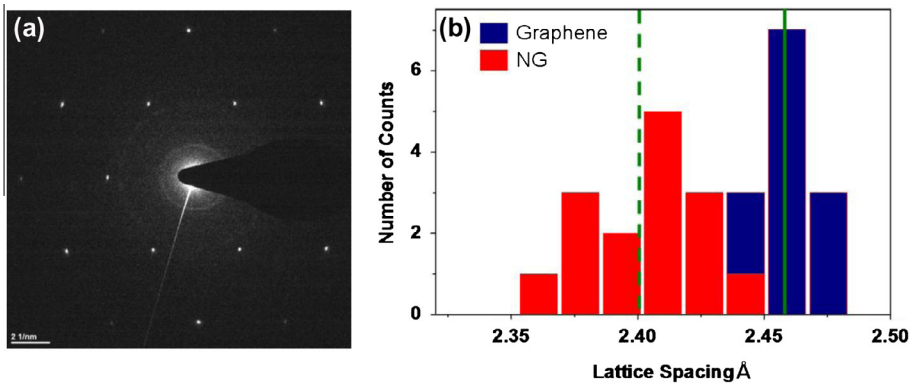

Fig. 5 – (a) Electron-diffraction patterns of NG by TEM. (b) Distribution of the lattice spacing *d* of different graphene and NG samples.

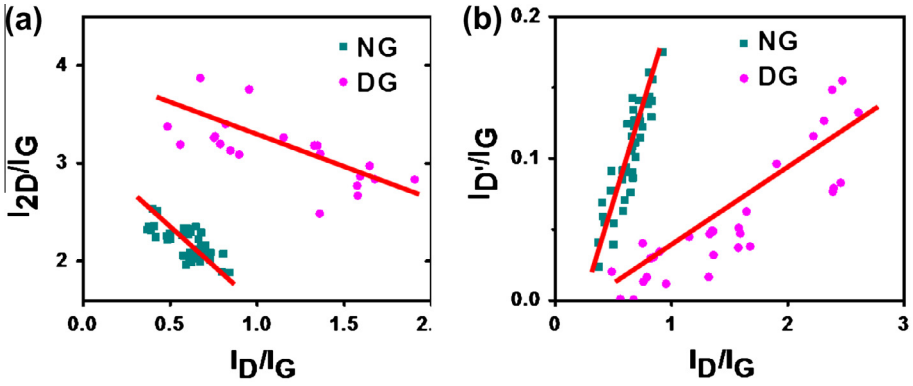

Fig. 6 – Comparison of the intensity ratios I_{2D}/I_G (a) and $I_{D'}/I_G$ (b) of DG and NG with the increase of I_D/I_G.

can be realized by fluorination, oxidation and hydrogenation, while grain boundaries exist at graphene/graphite edges and domain boundaries. It is reported that $I_D/I_{D'}$ is ~13 for sp^3-defects, ~7 for vacancy-like defects, and ~3.5 for domain boundaries [32]. Till now, no experimental work has been done on NG to study the nature of defects. The trend of $I_{D'}/I_G$ (amplitude intensity ratio) of NG and DG with the increase of I_D/I_G is shown in Fig. 6b. The maximum I_D/I_G of NG and DG is 1.2 and 3.3. It is clearly observed that the $I_{D'}/I_D$ ratio is different for these two samples, which indicates that the defects in these two samples have different natures. The $I_D/I_{D'}$ of DG is from 7–10, close to the value of vacancy-like defects observed in [32]. On the other hand, the $I_D/I_{D'}$ of NG is ~3.5, which is close to the value of boundary defects. The reason why nitrogen dopants in NG behave like boundary defects is still not fully understood. It could be related to the lattice distortion in Pyrrolic N structure.

4. Conclusions

Systematical Raman studies of NG were carried out. The C–N bonding configuration is found to be pure Pyrrolic N, which might be related to the H_2 rich growth conditions. Raman images show that the distribution of defects/nitrogen dopants is not homogenous. Our results also suggest that the G peak position and I_{2D}/I_G ratio cannot be simply taken as a fingerprint of doping concentration in NG. There is compressive strain in NG as verified by TEM. Finally, the type of defects in NG is probed and found that they are most likely boundary defects. The detail analysis of the Raman spectra of NG would greatly help on the characterization and future application of this novel material.

Acknowledgements

This work is supported by NSFC (11144001, 11104026), Program for New Century Excellent Talents in University (NCET-11-0094), and Natural Science Foundation of Jiangsu Province (BK2011585, BE2011159 and BK2012024), and Chinese postdoctoral fundings (No. 2012M520053).

REFERENCES

[1] Geim AK, Novoselov KS. The rise of graphene. Nat Mater 2007;6:183–91.
[2] Geim AK. Graphene: status and prospects. Science 2009;324:1530–4.
[3] Castro Neto AH, Guinea F, Peres NMR, Geim AK. The electronic properties of graphene. Rev Mod Phys 2009;81(1):109–62.
[4] Balandin AA. Thermal properties of graphene and nanostructured carbon materials. Nat Mater 2011;10:569–81.

[5] Zhan D, Yan JX, Lai LF, Ni ZH, Liu L, Shen ZX. Engineering the electronic structure of graphene. Adv Mater 2012;24(30):4055–69.
[6] Deifallah M, McMillan PF, Cora F. Electronic and structural properties of two-dimensional carbon nitride graphenes. J Phys Chem C 2008;112(14):5447–53.
[7] Martins TB, Miwa RH, da Silva AJR, Fazzio A. Electronic and transport properties of boron-doped graphene nanoribbons. Phys Rev Lett 2007;98:196803/1-/4.
[8] Wei DC, Liu YQ, Wang Y, Zhang HL, Huang LP, Yu G. Synthesis of N-doped graphene by chemical vapor deposition and its electrical properties. Nano Lett 2009;9(5):1752–8.
[9] Qu LT, Liu Y, Baek JB, Dai LM. Nitrogen-doped graphene as efficient metal-free electrocatalyst for oxygen reduction in fuel cells. ACS Nano 2010;4(3):1321–6.
[10] Zhao L, He R, Rim KT, Schiros T, Kim KS, Zhou H, et al. Visualizing individual nitrogen dopants in monolayer graphene. Science 2011;333:999–1003.
[11] Reddy ALM, Srivastava A, Gowda SR, Gullapalli H, Dubey M, Ajayan PM. Synthesis of nitrogen-doped graphene films for lithium battery application. ACS Nano 2010;4(11):6337–42.
[12] Zhong J, Yao J, Kittrell C, Tour JM. Large-scale growth and characterizations of nitrogen-doped monolayer graphene sheets. ACS Nano 2011;5(5):4112–7.
[13] Gao H, Song L, Guo WH, Huang L, Yang D, Wang F, et al. A simple method to synthesize continuous large area nitrogen-doped graphene. Carbon 2012;50(12):4476–82.
[14] Wang X, Li X, Zhang L, Yoon Y, Weber PK, Wang H, et al. N-doping of graphene through electrothermal reactions with ammonia. Science 2009;324:768–71.
[15] Jeong HM, Lee JW, Shin WH, Choi YJ, Shin HJ, Kang JK, et al. Nitrogen-doped graphene for high-performance ultracapacitors and the importance of nitrogen-doped sites at basal planes. Nano Lett 2011;11(6):2472–7.
[16] Lin YC, Lin CY, Chiu PW. Controllable graphene N-doping with ammonia plasma. Appl Phys Lett 2010;96:133110/1-/3.
[17] Wang Y, Shao Y, Matson DW, Li J, Lin Y. Nitrogen-doped graphene and its application in electrochemical biosensing. ACS Nano 2010;4(4):1790–8.
[18] Wang CD, Yuen MF, Ng TW, Jha SK, Lu ZZ, Kwok SY, et al. Plasma-assisted growth and nitrogen doping of graphene films. Appl Phys Lett 2012;100:253107/1-/5.
[19] Wang H, Maiyalagan T, Wang X. Review on recent progress in nitrogen-doped graphene: synthesis, characterization, and its potential applications. ACS Catal 2012;2(5):781–94.
[20] Zhang C, Fu L, Liu N, Liu M, Wang Y, Liu Z. Synthesis of nitrogen-doped graphene using embedded carbon and nitrogen sources. Adv Mater 2011;23(8):1020–4.
[21] Lv R, Li Q, Botello-Méndez Andérs R, Hayashi T, Wang B, Berkdemir A, et al. Nitrogen-doped graphene: beyond single substitution and enhanced molecular sensing. Sci Rep 2012;2:586/1-/8.
[22] Podila R, Chacón-Torres J, Spear JT, Pichler T, Ayala P, Rao AM. Spectroscopic investigation of nitrogen doped graphene. Appl Phys Lett 2012;101:123108/1-/4.
[23] Luo ZQ, Lim S, Tian Z, Shang J, Lai L, MacDonald B, et al. Pyridinic N-doped graphene: synthesis, electronic structure and electrocatalytic property. J Mater Chem 2011;21:8038–44.
[24] Malard LM, Pimenta MA, Dresselhaus G, Dresselhaus MS. Raman spectroscopy in graphene. Phys Rep 2009;473(5–6):51–87.
[25] Ni ZH, Ponomarenko LA, Nair RR, Yang R, Anissimova S, Grigorieva IV, et al. On resonant scatterers as a factor limiting carrier mobility in graphene. Nano Lett 2010;10:3868–72.
[26] Teweldebrhan D, Baladin AA. Modification of graphene properties due to electron-beam irradiation. Appl Phys Lett 2009;94:013101/1-/3.
[27] Liu G, Teweldebrhan D, Balandin AA. Tuning of graphene properties via controlled exposure to electron beams. IEEE Trans Nanotechnol 2011;10(4):865–70.
[28] Cancado LG, Jorio A, Martins Ferreira EH, Stavale F, Achete CA, Capaz RB, et al. Quantifying defects in graphene via Raman spectroscopy at different excitation energies. Nano Lett 2011;11(8):3190–6.
[29] Das A, Pisana S, Chakraborty B, Piscanec S, Saha SK, Waghmare UV, et al. Monitoring dopants by Raman scattering in an electrochemically top-gated graphene transistor. Nat Nanotechnol 2008;3:210–5.
[30] Ni ZH, Yu T, Luo ZQ, Wang YY, Liu L, Wong CP, et al. Probing charged impurities in suspended graphene using Raman spectroscopy. ACS Nano 2009;3(3):569–74.
[31] Ni ZH, Yu T, Lu YH, Wang YY, Feng YP, Shen ZX. Uniaxial strain on graphene: Raman spectroscopy study and bandgap opening. ACS Nano 2008;2(11):2301–5.
[32] Eckmann A, Felten A, Mishchenko A, Britnell L, Krupke R, Novoselov KS, et al. Probing the nature of defects in graphene by Raman spectroscopy. Nano Lett 2012;12(8):3925–30.
[33] Venezuela P, Lazzeri M, Mauri F. Theory of double-resonant Raman spectra in graphene: intensity and line shape of defect-induced and two-phonon bands. Phys Rev B 2011;84:035433/1-/25.
[34] Ferrari AC, Meyer JC, Scardaci V, Casiraghi C, Lazzeri M, Mauri F, et al. Raman spectrum of graphene and graphene layers. Phys Rev Lett 2006;97:187401/1-/4.
[35] Li X, Zhu Y, Cai W, Borysiak M, Han B, Chen D, et al. Transfer of large-area graphene films for high-performance transparent conductive electrodes. Nano Lett 2009;9(12):4359–63.
[36] Ni ZH, Wang HM, Kasim J, Fan HM, Yu T, Wu YH, et al. Graphene thickness determination using reflection and contrast spectroscopy. Nano Lett 2007;7(9):2758–63.
[37] Maciel IO, Anderson N, Pimenta MA, Hartschuh A, Qian HH, Terrones M, et al. Electron ans phonon renormalization near charged defects in carbon nanotubes. Nat Mater 2008;7:878–83.
[38] Ni ZH, Wang HM, Ma Y, Johnson K, Wu YH, Shen ZX. Tunable stress and controlled thickness modification in graphene by annealing. ACS Nano 2008;2(5):1033–9.
[39] Dettori R, Cadelano E, Colombo L. Elastic fields and moduli in defected graphene. J Phys: Condens Matter 2012;24(10):104020/1-/10.
[40] Allen FH, Kennard O, Watson DG, Brammer L, Orpen AG, Taylor R. Tables of bond lengths determined by X-ray and neutron diffraction. Part 1. Bond lengths in organic compounds. J Chem Soc, Perkin Trans 2 1987;12:S1–S19.
[41] Yu V, Whiteway E, Maassen J, Hilke M. Raman spectroscopy of the internal strain of a graphene layer grown on copper tuned by chemical vapor deposition. Phys Rev B 2011;84:205407.